J|A|C|S
ARTICLES
Published on Web 01/05/2007

Strengths of Hydrogen Bonds Involving Phosphorylated Amino Acid Side Chains

Daniel J. Mandell,[†] Ilya Chorny,[‡] Eli S. Groban,[§] Sergio E. Wong,[§] Elisheva Levine,[||] Chaya S. Rapp,[||] and Matthew P. Jacobson*,[‡]

Contribution from the Graduate Program in Biological and Medical Informatics, Department of Pharmaceutical Chemistry, and Graduate Group in Biophysics, University of California, San Francisco, California 94143, and Department of Chemistry, Stern College for Women, Yeshiva University, New York, New York 10016

Received May 1, 2006; E-mail: matt.jacobson@ucsf.edu

Abstract: Post-translational phosphorylation plays a key role in regulating protein function. Here, we provide a quantitative assessment of the relative strengths of hydrogen bonds involving phosphorylated amino acid side chains (pSer, pAsp) with several common donors (Arg, Lys, and backbone amide groups). We utilize multiple levels of theory, consisting of explicit solvent molecular dynamics, implicit solvent molecular mechanics, and quantum mechanics with a self-consistent reaction field treatment of solvent. Because the ~6 pKa of phosphate suggests that −1 and −2 charged species may coexist at physiological pH, hydrogen bonds involving both protonated and deprotonated phosphates for all donor−acceptor pairs are considered. Multiple bonding geometries for the charged−charged interactions are also considered. Arg is shown to be capable of substantially stronger salt bridges with phosphorylated side chains than Lys. A pSer hydrogen-bond acceptor tends to form more stable interactions than a pAsp acceptor. The effect of phosphate protonation state on the strengths of the hydrogen bonds is remarkably subtle, with a more pronounced effect on pAsp than on pSer.

Protein phosphorylation is a key signaling mechanism in diverse cellular processes including metabolism,[1] ion channel regulation,[2,3] and cell cycle progression.[4−6] In eukaryotes, the main sites of phosphorylation are tyrosine, serine, and threonine side chains, while aspartate and histidine side chains are phosphorylated in the "two-component" signaling pathways of prokaryotes.[6,7] Addition of the phosphate group, which typically carries a −2 charge at physiological pH, perturbs the local electrostatic potential in the protein and often induces conformational changes that influence function[6] or modulate protein−protein interactions.[1]

A critical property of phosphorylated residues is their propensity to accept hydrogen bonds through their phosphate oxygens, frequently with positively charged side chains to form "salt bridges". Salt bridge energetics depend sensitively on the identity, proximity, and orientation of the participating side chains and their surrounding environment. Quantitative measurements of salt bridge contributions to protein stability have provided different results depending on the experimental system and experimental design, with estimates ranging from −5.0 to −0.5 kcal/mol of stabilization in T4 lysozyme,[8,9] to 2.0 to 4.0 kcal/mol of destabilization in coiled coils and Arc repressor.[10,11] There have also been a number of previous computational studies aimed at quantifying the strength of interaction of small ions.[12−15] In particular, Masunov and Lazaridis[15] used molecular dynamics methods to estimate the free energies of salt bridges between likely orientations of all charged naturally occurring amino acid side chains.

This work investigates the strengths of hydrogen bonds and salt bridges involving phosphorylated amino acid side chains using small molecule analogues for common acceptors (methyl phosphate for pSer and pThr, acetyl phosphate for pAsp) and donors (butyl ammonium for a Lys side chain, propyl guanini-dinium for Arg, and *N*-methylacetamide for backbone amide

[†] Graduate Program in Biological and Medical Informatics, University of California, San Francisco.
[‡] Department of Pharmaceutical Chemistry, University of California, San Francisco.
[§] Graduate Group in Biophysics, University of California, San Francisco.
[||] Yeshiva University.

(1) Audette, G. F.; Engelmann, R.; Hengstenberg, W.; Deutscher, J.; Hayakawa, K.; Quail, J. W.; Delbaere, L. T. *J. Mol. Biol.* **2000**, *303*, 545−53.
(2) Patel, A. J.; Honore, E. *Trends Neurosci.* **2001**, *24*, 339−46.
(3) Martens, J. R.; Kwak, Y. G.; Tamkun, M. M. *Trends Cardiovasc. Med.* **1999**, *9*, 253−8.
(4) Vermeulen, K.; Van Bockstaele, D. R.; Berneman, Z. N. *Cell Prolif.* **2003**, *36*, 131−49.
(5) Feng, M. H.; Philippopoulos, M.; MacKerell, A. D.; Lim, C. *J. Am. Chem. Soc.* **1996**, *118*, 11265−11277.
(6) Johnson, L. N.; Lewis, R. J. *Chem. Rev.* **2001**, *101*, 2209−2242.
(7) Johnson, L. N.; Oreilly, M. *Curr. Opin. Struct. Biol.* **1996**, *6*, 762−769.
(8) Anderson, D. E.; Becktel, W. J.; Dahlquist, F. W. *Biochemistry* **1990**, *29*, 2403−2408.
(9) Sun, D. P.; Sauer, U.; Nicholson, H.; Matthews, B. W. *Biochemistry* **1991**, *30*, 7142−53.
(10) Schneider, J. P.; Lear, J. D.; DeGrado, W. F. *J. Am. Chem. Soc.* **1997**, *119*, 5742−5743.
(11) Waldburger, C. D.; Schildbach, J. F.; Sauer, R. T. *Nat. Struct. Biol.* **1995**, *2*, 122−128.
(12) Lyubartsev, A. P.; Laaksonen, A. *Phys. Rev. E* **1997**, *55*, 5689−5696.
(13) Martorana, V.; La Fata, L.; Bulone, D.; San Biagio, P. L. *Chem. Phys. Lett.* **2000**, *329*, 221−227.
(14) Luo, R.; David, L.; Hung, H.; Devaney, J.; Gilson, M. K. *J. Phys. Chem. B* **1999**, *103*, 727−736.
(15) Masunov, A.; Lazaridis, T. *J. Am. Chem. Soc.* **2003**, *125*, 1722−1730.

10.1021/ja063019w CCC: $37.00

NH groups). Interactions of all donors with propionic acid (Glu analogue) are also considered for comparison to a carboxylate receptor with −1 charge.

We utilize multiple levels of theory, including explicit solvent molecular dynamics (MD), implicit solvent molecular mechanics (Poisson−Boltzmann), and quantum mechanics with a self-consistent reaction field treatment of solvent. This approach allows us to identify trends that are consistent across the methods, as well as uncover the sensitivity of each method to different forces governing hydrogen-bond strengths. Continuum solvent methods, primarily those based on the Poisson−Boltzmann equation[16] or more heuristic methods such as Generalized Born,[17] offer substantial speed advantages relative to explicit solvent models in applications such as molecular dynamics. However, treating the solvent as a continuum dielectric is an approximation and neglects important first-shell solvation effects related to the finite size and asymmetry of a water molecule.[18−20] The results of the explicit solvent calculations cannot be considered free of error either. Notably, molecular mechanics methods using fixed-charged force fields, as employed in the present molecular dynamics calculations, ignore the effect of electronic polarizability on hydrogen-bond strengths. Even in high dielectric solvent, the strong electric field exerted by a −2 phosphate group can be expected to lead to significant polarization of the electrons on nearby molecules. To assess the potential impact of electronic polarizability on the strengths of the hydrogen bonds considered here, we have used quantum mechanics with a large basis set, electron correlation treated at the "local" Moller−Plesset second-order perturbation theory[21] (LMP2) level, and solvent treated using a self-consistent reaction field (SCRF) method.

The central results of this work consist of potentials of mean force (PMFs) from the explicit solvent molecular dynamics calculations, which are one-dimensional free energy landscapes for a pair of interacting groups as a function of distance between the phosphate and hydrogen-bond donors. The PMFs cannot be used trivially to predict the absolute free energies of association of the small molecules in solution (which requires extensive averaging over translational and rotational degrees of freedom) or the absolute strengths of hydrogen bonds in a protein environment (which depend on the local environment, such as solvent accessibility). However, the PMFs do provide insight into the relative intrinsic strengths of the various types of hydrogen bonds considered and help to address the following issues.

(1) The first issue concerns the conditions under which Arg or Lys make stronger hydrogen bonds with a phosphorylated side chain. There is ample albeit indirect evidence that the ability of guanidinium ions to form bidentate hydrogen bonds with carboxylate or phosphate ions leads to particularly strong interactions.[22−24] This property of guanidinium ions has been extensively employed in the design of synthetic receptors for phosphate-containing ligands.[25] Bidentate hydrogen bonds between Arg and pSer/pThr are also commonly observed in the relatively small number of crystal structures of phosphorylated proteins.[6] However, previous computational studies have suggested that interactions of phosphorylated groups with Lys may be intrinsically stronger.[26,27] We revisit this issue here using multiple levels of theory.

(2) The next issue is the effect of phosphate protonation state on hydrogen-bond strength. The ∼6 pKa of phosphate suggests that both −1 and −2 charged species may coexist at physiological pH. We investigate the effect of phosphate protonation state on all hydrogen-bonding interactions considered.

(3) The final issue concerns the energetic consequences of substituting a carboxylate for a phosphate. In cases where phosphorylation of a protein leads to its activation, it is frequently useful to engineer a constitutively active mutant, for example, for use in in vitro studies. Simply substituting a Glu or Asp for the phosphorylated residue(s) is sufficient to achieve constitutive activation in many cases,[28−32] but in other cases this simple strategy results in only partial activation or none at all.[33,34] The relative strengths of hydrogen bonds involving carboxylates and phosphates are also relevant to the design of inhibitors of SH2 domains,[35,36] which bind phosphorylated peptides. Here, we examine in some detail the differences in the intrinsic hydrogen-bond strengths of carboxylates versus phosphates with common hydrogen-bond donors. These results provide a foundation for understanding why Asp/Glu can sometimes substitute for phosphorylated amino acids, although other physicochemical differences will undoubtedly also play a role.

We do not directly address the strengths of hydrogen bonds to the phosphate backbone of RNA[37] and DNA,[38] although the results we present may have some relevance to this issue.

Materials and Methods

MD Simulation Materials and Parameters. MD simulations were performed using GROMACS 3.2.1.[39] The 2001 OPLS all-atom force field[40] was used for stretch, bend, torsional, and Lennard-Jones parameters, as well as partial charges for the glutamate, acetate, arginine,

(16) Gilson, M. K. *Curr. Opin. Struct. Biol.* **1995**, *5*, 216−223.
(17) Ghosh, A.; Rapp, C. S.; Friesner, R. A. *J. Phys. Chem. B* **1998**, *102*, 10983−10990.
(18) Chorny, I.; Dill, K. A.; Jacobson, M. P. *J. Phys. Chem. B* **2005**, *109*, 24056−24060.
(19) Asthagiri, D.; Schure, M. R.; Lenhoff, A. M. *J. Phys. Chem. B* **2000**, *104*, 8753−8761.
(20) Yu, Z.; Jacobson, M. P.; Rapp, C. S.; Friesner, R. A. *J. Chem. Phys.* **2004**, *108*, 6643−6654.
(21) Saebo, S.; Pulay, P. *Annu. Rev. Phys. Chem.* **1993**, *44*, 213−236.
(22) Singh, J.; Thornton, J. M.; Snarey, M.; Campbell, S. F. *FEBS Lett.* **1987**, *224*, 161−171.
(23) Saenger, W.; Wagner, K. G. *Acta Crystallogr.* **1972**, *B28*, 2237−2244.
(24) Lewin, S. *J. Theor. Biol.* **1969**, *23*, 279−284.
(25) Schug, K. A.; Lindner, W. *Chem. Rev.* **2005**, *105*, 67−113.
(26) Mavri, J.; Vogel, H. J. *Proteins: Struct., Funct., Genet.* **1996**, *24*, 495−501.
(27) Deerfield, D. W.; Nicholas, H. B.; Hiskey, R. G.; Pedersen, L. G. *Proteins: Struct., Funct., Genet.* **1989**, *6*, 168−192.
(28) Charbon, G.; Breunig, K. D.; Wattiez, R.; Vandenhaute, J.; Noel-Georis, I. *Mol. Cell. Biol.* **2004**, *24*, 4083−91.
(29) Kassenbrock, C. K.; Anderson, S. M. *J. Biol. Chem.* **2004**, *279*, 28017−27.
(30) Huang, W.; Erikson, R. L. *Proc. Natl. Acad. Sci. U.S.A.* **1994**, *91*, 8960−3.
(31) Klose, K. E.; Weiss, D. S.; Kustu, S. *J. Mol. Biol.* **1993**, *232*, 67−78.
(32) McCabe, T. J.; Fulton, D.; Roman, L. J.; Sessa, W. C. *J. Biol. Chem.* **2000**, *275*, 6123−8.
(33) Zhang, J.; Zhang, F.; Ebert, D.; Cobb, M. H.; Goldsmith, E. J. *Structure* **1995**, *3*, 299−307.
(34) Mansour, S. J.; Candia, J. M.; Matsuura, J. E.; Manning, M. C.; Ahn, N. G. *Biochemistry* **1996**, *35*, 15529−36.
(35) Garcia-Echeverria, C. *Curr. Med. Chem.* **2001**, *8*, 1589−1604.
(36) Cody, W. L.; Lin, Z. W.; Panek, R. L.; Rose, D. W.; Rubin, J. R. *Curr. Pharm. Des.* **2000**, *6*, 59−98.
(37) Calnan, B. J.; Tidor, B.; Biancalana, S.; Hudson, D.; Frankel, A. D. *Science* **1991**, *252*, 1167−71.
(38) Frigyes, D.; Alber, F.; Pongor, S.; Carloni, P. *J. Mol. Struct. (THEOCHEM)* **2001**, *574*, 39−45.
(39) Van Der Spoel, D.; Lindahl, E.; Hess, B.; Groenhof, G.; Mark, A. E.; Berendsen, H. J. *J. Comput. Chem.* **2005**, *26*, 1701−18.
(40) Kaminski, G. A.; Friesner, R. A.; Tirado-Rives, J.; Jorgensen, W. L. *J. Phys. Chem. B* **2001**, *105*, 6474−6487.

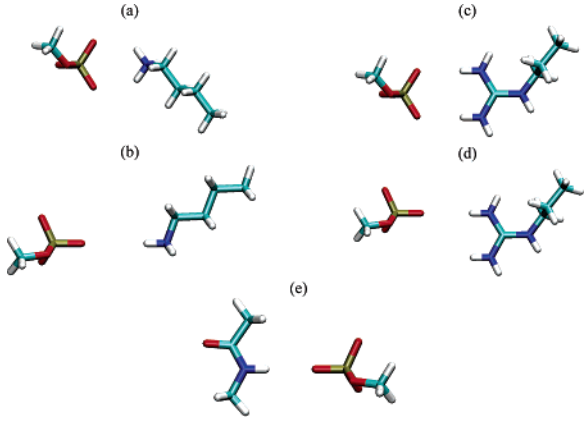

Figure 1. Hydrogen-bonding geometries considered in this work. Only the unprotonated methyl phosphate acceptor (representing the pSer side chain with a −2 charge) is shown. In the case of protonated phosphate groups, the hydrogen is placed on one of the oxygens not directly involved in hydrogen bonding. We refer to these geometries as (a) "Lys coplanar", (b) "Lys collinear", (c) "Arg coplanar", (d) "Arg collinear", and (e) "amide NH collinear".

lysine, and *N*-methylacetamide backbone analogues. Partial charges for pSer (−1, −2) and pAsp (−1, −2) analogues were obtained from quantum mechanical calculations,[41,42] and these are presented together with the phosphate OPLS atom types in the Supporting Information. Molecules were solvated with TIP3P[43] water molecules in a 40 Å cubic box under periodic boundary conditions. The cutoff distance for the short-range neighbor list was set to 10 Å. Long-range electrostatics were calculated with particle mesh Ewald[44] with a real-space cutoff of 9 Å for nonbonded interactions. Na^+ counterions were fixed at the corners of the solvent box as necessary to obtain electroneutrality. Prior to running molecular dynamics, the potential energy of each configuration was relaxed by steepest descent minimization, followed by 100 ps of molecular dynamics equilibration. Molecular dynamics was then run for 2.1 ns with a time step of 2 fs. Interaction energies and atomic coordinates were recorded every 500 fs. The system was propagated in time with a velocity version of the Verlet algorithm.[45,46] During and subsequent to equilibration, Nose−Hoover temperature coupling[47] and Berendsen pressure coupling[48] were used to maintain system temperature and pressure, with a reference temperature of 298 K, a reference pressure of 1.0 atm, a time constant of 1 ps, and an isothermal compressibility of 1.1×10^{-6} (kcal mol^{-1} Å^{-3}). The various acceptors, donors, charge states, and geometries comprised a total of 25 hydrogen-bonding configurations, representing more than 1 μs of molecular dynamics simulation time.

MD Simulation Constraints. Umbrella sampling[49] using distance and position restraints was employed to calculate a one-dimensional PMF for one of two common interaction geometries, either a coplanar approach or a collinear approach (Figure 1). These orientations consistently arose in simulations of the side-chain analogues without position restraints (data not shown). For collinear geometries, the donated hydrogen and its covalently bonded atom, and the accepting oxygen and its covalently bonded atom, were constrained to move on a line. For coplanar geometries, donated hydrogens and accepting oxygens were constrained to a plane, and two additional heavy atoms from each molecule were constrained to move along a line. These constraints kept the interacting moieties facing each other, and in the case of lysine allowed the donated hydrogens to rotate slightly through the plane of interaction to sample optimal hydrogen-bonding orientations. Hydrogen atom−heavy atom covalent bond lengths were constrained only in the backbone analogue using the LINCS algorithm[50] to stabilize the N−H bond.

The distance between the molecules was constrained using a biasing potential at 0.5 Å intervals. A nearby heavy atom from the donor molecule was constrained to that of the acceptor using a quadratic biasing potential,

$$V(r) = k(r - r_i) \tag{1}$$

where $k = 143.5$ (kcal/Å^2) is the biasing force constant and r_i is the point about which the molecules are constrained. In cases with guanidinium in a coplanar orientation, additional simulation with a higher force constant of 263.0, 430.4, or 860.8 (kcal/Å^2) was necessary to sample adequately around the solvation barrier.

MD Analysis. The potential of mean force was calculated using probability distributions of the constrained distance, *r*, obtained from the umbrella sampling, as described by Souaille and Roux.[51] Trajectories from each window *i* were converted to biased population distributions $P_i(r)$ with a bin width of 0.1 Å. The weighted histogram analysis method (WHAM)[52] was used to merge histograms $P_i(r)$ into a single unbiased curve $P(r)$. The algorithm was considered to converge after the free energy constants for all of the windows changed by less with 0.01 kcal/mol. The PMF, $\Delta G(r)$, was then calculated using the standard relationship

$$\Delta G(r) = -k_b T \ln[P(r)] \tag{2}$$

where k_b is Boltzmann's constant. Each PMF was shifted vertically so that the average potential between 10 and 11 Å was 0 kcal/mol. Block averaging[53] was used to calculate errors. The trajectories in each of the constrained windows were divided into *N* shorter trajectories. The distribution $P(r)$ for each of the *N* trajectories was then calculated using the methods described above. The resulting *N* $P(r)$ were averaged and used to calculate the standard deviation, which we report as the error. $N = 20$ was chosen to minimize the correlation between neighboring blocks.

Implicit Solvent Continuum Electrostatics. Implicit solvent calculations were performed using the DelPhi program[54] to solve the linearized Poisson−Boltzmann equation. To compare with the explicit solvent PMFs, DelPhi calculations were performed on each configuration used in the MD simulations except that the molecules were fixed at a defined distance from 2.5 to 11.0 Å at 0.25 Å intervals. The Coulombic and solvation (reaction field) components of the free energy from DelPhi were added to Lennard-Jones energies calculated separately to obtain the implicit solvent PMF. The nonpolar component of the solvation free energy was computed with a solvent-accessible surface area model. The partial charges and atomic radii in the explicit and implicit solvent simulations were the same; that is, we did not use the default charges and radii from Delphi, to compare more directly with the molecular dynamics results. The Delphi calculations used 4 grid points per Å, an internal dielectric of 1, an external dielectric of 80, and an ionic strength of zero.

(41) Wong, S. E.; Bernacki, K.; Jacobson, M. P. *J. Phys. Chem. B* **2005**, *109*, 5249−5258.
(42) Groban, E. S.; Narayanan, A.; Jacobson, M. P. *PLoS Comput. Biol.* **2006**, *2*, 534−553.
(43) Jorgensen, W. L.; Chandrasekhar, J.; Madura, J. D.; Impey, R. W.; Klein, M. L. *J. Chem. Phys.* **1983**, *79*, 926−935.
(44) Darden, T.; York, D.; Pedersen, L. *J. Chem. Phys.* **1993**, *98*, 10089−10092.
(45) Swope, W. C.; Andersen, H. C.; Berens, P. H.; Wilson, K. R. *J. Chem. Phys.* **1982**, *76*, 637−649.
(46) Verlet, L. *Phys. Rev.* **1967**, *159*, 98.
(47) Hoover, W. G. *Phys. Rev. A* **1985**, *31*, 1695−1697.
(48) Berendsen, H. J. C.; Postma, J. P. M.; Vangunsteren, W. F.; Dinola, A.; Haak, J. R. *J. Chem. Phys.* **1984**, *81*, 3684−3690.
(49) Torrie, G. M.; Valleau, J. P. *J. Comput. Phys.* **1977**, *23*, 187−199.
(50) Hess, B.; Bekker, H.; Berendsen, H. J. C.; Fraaije, J. G. E. M. *J. Comput. Chem.* **1997**, *18*, 1463−1472.
(51) Souaille, M.; Roux, B. *Comput. Phys. Commun.* **2001**, *135*, 40−57.
(52) Kumar, S.; Bouzida, D.; Swendsen, R. H.; Kollman, P.; Rosenberg, J. M. *J. Comput. Chem.* **1992**, *13*, 1011−1021.
(53) Allen, M. P.; Tildesley, D. J. *Computer Simulation of Liquids*; Oxford University Press: New York, 1989.
(54) Nicholls, A.; Honig, B. *J. Comput. Chem.* **1991**, *12*, 435−445.

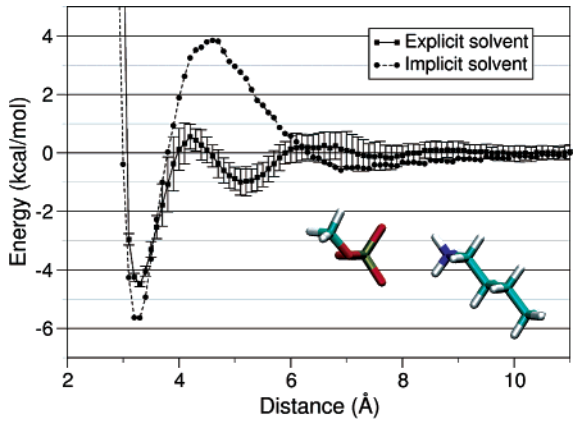

Figure 2. PMFs for a coplanar interaction between methyl phosphate (representing $pSer^{-2}$) and butyl ammonium (Lys) computed using MD in explicit solvent (squares with error bars, computed as described in Materials and Methods), and using molecular mechanics with implicit solvent (dotted line and circles). The distance along the *x*-axis is measured between the phosphorus atom and the ammonium nitrogen. The PMFs for the other 24 hydrogen-bonding interactions are available in the Supporting Information.

Quantum Mechanics. Quantum mechanics calculations were performed using the Jaguar software package.[55] Ab initio single-point energy calculations were performed on the same coordinates employed for the implicit solvent molecular mechanics results. A self-consistent reaction field (SCRF) method[56] was used to mimic the condensed phase environment. The procedure started by calculating atomic charges for the molecule in a vacuum using electrostatic fitting.[57,58] This step entailed a Hartree−Fock calculation and subsequent electron correlation correction to evaluate the electrostatic potential. The response from the surrounding dielectric and corresponding surface charges was calculated. Atomic charges were then recalculated taking into account the dielectric response. The solvation energy was calculated at each iteration until it converged. The basis set for the Hartree−Fock and electron correlation calculations was cc-pVTZ(-f). Electron correlation was treated at the level of local Moller−Plesset second-order perturbation theory (LMP2).[21]

Results and Discussion

Each level of theory employed in this study captures different aspects of hydrogen bonding with varying computational expense. Although not free from error, the explicit solvent molecular dynamics results include substantial averaging over conformational and rotational degrees of freedom for both solute and solvent, and comprise the core of our results. Our explicit solvent PMFs take a form typical for those of oppositely charged ions (e.g., Figure 2). The lowest free energy is generally seen when the ions are directly in contact (separation distance roughly equal to the sum of the van der Waals radii); we refer to this minimum as the "contact minimum". As the separation between the ions increases, the free energy rises sharply to a solvation barrier. In many cases, as the separation between the molecules increases further, the free energy reaches a second minimum, in which the solute ions are separated by approximately one water molecule, which we refer to as the "solvent-separated minimum". In cases with particularly well-ordered waters, a second barrier and second solvent-separated minimum may exist with further separation. At distances beyond these features, the potential energy approaches zero. The free energy of the hydrogen bond or salt bridge is calculated as the difference in energy between the largest separation sampled (11 Å) and the contact minimum. The free energies of all orientations, charge states, and acceptor−donor pairs as calculated by MD in explicit solvent are summarized in Table 1.

Control Study of NaCl. As a control, we computed a one-dimensional PMF between Na^+ and Cl^- ions (Supporting Information), a very well-studied system. This experiment allowed for comparisons to previous studies without the rotational degrees of freedom and multiple partial charges inherent to polyatomic systems. Our calculations yielded a free energy at the contact minimum of −1.7 kcal/mol and a free energy at the top of the solvation barrier of 1.7 kcal/mol. Masunov and Lazaridis[15] found a contact minimum free energy of about −1.3 kcal/mol and a solvation barrier free energy of about 2.0 kcal/mol when using a Spherical Solvent Boundary Potential[59] for long-range electrostatics, and −2.0 and 1.5 kcal/mol, respectively, for the free energy when using Ewald summation. Other comparable studies from Smith and Deng,[60] Lyubartsev and Laaksonen[12] (at 0.5 M concentration), and Martorana et al.[13] found comparable results, with contact minima of about −1 to −2 kcal/mol.

Effect of Interaction Geometry on Energy Landscapes. Examples of the collinear and coplanar geometries used for the PMFs are depicted in Figure 1. In cases where the phosphate is protonated, the proton is placed on an oxygen not involved in the hydrogen bonding; it serves only to change the overall charge on the phosphate. In the coplanar orientation, the molecules are constrained to move along the axis of the distance constraint, and the planarity constraint prevents rotation about this axis. In contrast, the collinear orientation allows for rotation about the collinear axis. The height of the solvation barriers and the stability of the solvent-separated minima depend on the relative rotation of the molecules about the collinear axis, so by integrating out this degree of freedom we produce PMFs with less pronounced maxima, and frequently no secondary minima, in comparison to the coplanar PMFs (all PMFs are available in the Supporting Information). Note that the free energy computed for the hydrogen bond in this type of PMF explicitly includes entropic contributions from rotations about the collinear axis.

Salt Bridge Interactions of Glu/Asp. The strengths of salt bridges between positively charged Lys or Arg with negatively charged carboxylate groups on Glu and Asp have been considered in several previous studies.[15,61] We include our own data here only to obtain an internally consistent comparison with the results involving phosphate groups. Taking a collinear approach, propyl guanidinium (Arg) and butyl ammonium (Lys) yield similar free energies when donating hydrogen bonds to propionic acid (Glu), at −3.4 and −3.1 kcal/mol, respectively. In a planar approach, Arg is much more stable, at −8.5 kcal/mol. The enhanced stability of Arg is largely due to the ability of its guanidinium moiety to form nearly idealized bidentate

(55) *Jaguar*, 5.0; Schrodinger, L. L. C.: Portland, OR, 1991−2003.
(56) Tannor, D. J.; Marten, B.; Murphy, R.; Friesner, R. A.; Sitkoff, D.; Nicholls, A.; Ringnalda, M.; Goddard, W. A.; Honig, B. *J. Am. Chem. Soc.* **1994**, *116*, 11875−11882.
(57) Chirlian, L. E.; Francl, M. M. *J. Comput. Chem.* **1987**, *8*, 894−905.
(58) Woods, R. J.; Khalil, M.; Pell, W.; Moffat, S. H.; Smith, V. H. *J. Comput. Chem.* **1990**, *11*, 297−310.
(59) Beglov, D.; Roux, B. *J. Chem. Phys.* **1994**, *100*, 9050−9063.
(60) Smith, D. E.; Dang, L. X. *J. Chem. Phys.* **1994**, *100*, 3757−3766.
(61) Rozanska, X.; Chipot, C. *J. Chem. Phys.* **2000**, *112*, 9691−9694.

Table 1. Hydrogen-Bonding Free Energies with Standard Errors in kcal/mol Computed from Explicit Solvent MD and WHAM

	Lys collinear	Arg collinear	Lys coplanar	Arg coplanar	amide NH collinear
Glu	-3.1 ± 0.3	-3.4 ± 0.2	-2.6 ± 0.4	-8.5 ± 0.1	-1.8 ± 0.6
pSer(−1)	-3.7 ± 0.2	-3.7 ± 0.3	-3.5 ± 0.1	-9.3 ± 0.4	-1.6 ± 0.7
pSer(−2)	-4.2 ± 0.3	-4.7 ± 0.3	-4.5 ± 0.3	-10.6 ± 0.6	-1.0 ± 0.6
pAsp(−1)	-3.2 ± 0.3	-3.0 ± 0.4	-2.4 ± 0.4	-6.3 ± 0.4	-1.8 ± 0.7
pAsp(−2)	-4.6 ± 0.2	-4.5 ± 0.3	-4.9 ± 0.4	-7.3 ± 0.2	-1.1 ± 0.6

hydrogen bonds with the carboxylate moiety of Glu. Moreover, the free energy of the bidentate bonds is slightly greater than double that of the single collinear bond, suggesting some cooperativity as there is less of an entropic cost to pay in forming the second hydrogen bond. Entropic cooperativity in bidentate bonding interactions, sometimes referred to as the chelate effect, has been observed elsewhere experimentally.[62]

Masunov and Lazaridis computed one-dimensional PMFs between ionizable side-chain analogues similar to the configurations we have used.[15] In particular, our Glu−Arg coplanar approach (Supporting Information) used ionic structures and positional restraints similar to those employed by Masunov and Lazaridis in a corresponding calculation. Their analysis yielded a contact minimum free energy and solvation barrier free energy of about −4.3 and 3.0 kcal/mol, respectively, roughly one-half the magnitude of our results. This discrepancy is likely attributable to differences in force fields and simulation protocol. Importantly, their simulations were run with the CHARMM 19 force field[63] for side-chain analogues, while ours used the OPLS-AA 2001 force field (see Materials and Methods). Notably, the charges for the donated Arg hydrogens are 0.35*e* in CHARMM as opposed to 0.46*e* in OPLS, and the accepting Glu oxygens take a charge of −0.60*e* in CHARMM in contrast to −0.80*e* in OPLS. Further, Masunov and Lazaridis handled long-range electrostatics with a Spherical Solvent Boundary Potential[59] (SSBP) over a spherical cluster of 200 waters with an 11 Å radius, while we employed particle mesh Ewald over a 40 Å cubic box of roughly 2150 water molecules. Figure 2 of the Masunov paper shows that SSBP produces a contact minimum about 0.7 times the depth as Ewald summation when calculating a one-dimensional PMF for Na^+ and Cl^- ions. Rodinger et al.[64] found that the interface between an explicit water droplet and a continuum solvent field appearing in models like SSBP polarizes the explicit waters up to 10 Å away from the solvent−vacuum boundary. Lattice summation methods like particle mesh Ewald can also introduce small artifacts related to periodicity-induced perturbations in Coulombic and solvation energies, although given the quantity and permittivity of the solvent in the present study these perturbations should nearly cancel each other.[65] Additionally, the earlier paper reports the typical use of 7 umbrella sampling windows constructed at 1 Å intervals from 3 to 9 Å and simulated for 200 ps. In the present study, 18 windows were used, ranging from 2.5 to 11 Å at 0.5 Å intervals, and each window was equilibrated for 200 ps followed by 2.1 ns of simulation.

Rozanska and Chipot[61] calculated a PMF for guanidinium and acetate using Ewald lattice summation for long-range electrostatics, which corresponds geometrically to our Glu−Arg coplanar orientation. Their simulations produced a contact minimum free energy of −2.7 kcal/mol and a solvation barrier free energy of 3.4 kcal/mol. The atomic partial charges were computed from quantum mechanics and more closely resembled those of OPLS than CHARMM, with the donated hydrogens at 0.49*e* and the accepting oxygens at −0.87*e*. Importantly, their guanidinium and acetate moieties were biased to face one another through torsional restraints. This would allow some degree of rotation through the plane of interaction, in contrast to the C−C−C−N linearity constraint imposed on the corresponding ions of the present study, which enforces nearly constant bidentate hydrogen bonding. We have found that removing this linearity constraint reduces the stability of the salt bridge by at least 1.5 kcal/mol. Other notable differences include Rozanska and Chipot's use of 4 umbrella sampling windows rather than 18, the AMBER force field[66] for the potential energy function rather than OPLS-AA, and the TIP4P water model rather than TIP3P.

Salt Bridge Interactions of pSer. We now turn our attention to hydrogen-bond interactions involving phosphorylated amino acid acceptors, the central results of this work. As is the case with carboxylate serving as the acceptor ion, butyl ammonium (Lys) and propyl guanidinium (Arg) donors yield similar contact minima free energies in a collinear orientation with protonated methyl phosphate ($pSer^{-1}$), at −3.7 kcal/mol. When pSer is deprotonated, the energies of the collinear orientation become more distinguishable, with $pSer^{-2}$−Arg forming a salt bridge worth −4.7 kcal/mol, as compared to −4.2 kcal/mol for $pSer^{-2}$−Lys. In the planar approach, Lys and Arg produce substantially different free energy profiles. When the accepting pSer is protonated, the contact minimum reaches −9.3 kcal/mol with Arg. If pSer takes a −2 charge, the free energy for this geometry is −10.6 kcal/mol.

The depth of the pSer−Arg contact minima further demonstrates the significance of bidentate hydrogen bonding in a coplanar approach. Similar to the effects observed with Glu−Arg, a coplanar pSer−Arg salt bridge provides more than twice the stability of one that is collinear. Coplanar pSer−Lys salt bridges yield energies similar to their collinear counterparts, which was also observed with Glu−Lys. PMFs with all permutations of pSer charge states with different donors also suggest that the effects of pSer protonation are small but significant. In a collinear approach, deprotonation of pSer stabilizes a pSer−Lys salt bridge by −0.5 kcal/mol and pSer−Arg by −1.0 kcal/mol. The effect appears stronger in a coplanar approach, with deprotonation stabilizing pSer−Lys by −1.0 kcal/mol and pSer−Arg by −1.3 kcal/mol.

(62) Breslow, R.; Belvedere, S.; Gershell, L.; Leung, D. *Pure Appl. Chem.* **2000**, *72*, 333−342.
(63) Brooks, B. R.; Bruccoleri, R. E.; Olafson, B. D.; States, D. J.; Swaminathan, S.; Karplus, M. *J. Comput. Chem.* **1983**, *4*, 187−217.
(64) Rodinger, T.; Howell, P. L.; Pomes, R. *J. Chem. Phys.* **2005**, *123*.
(65) Hunenberger, P. H.; McCammon, J. A. *Biophys. Chem.* **1999**, *78*, 69−88.
(66) Cornell, W. D.; Cieplak, P.; Bayly, C. I.; Gould, I. R.; Merz, K. M.; Ferguson, D. M.; Spellmeyer, D. C.; Fox, T.; Caldwell, J. W.; Kollman, P. A. *J. Am. Chem. Soc.* **1995**, *117*, 5179−5197.

Mavri and Vogel[26] used PM3 semiempirical molecular orbital calculations with the SM3 reaction field treatment of solvent[67] to investigate the strengths of interactions for methylammonium and methylguanadinium with mono- and divalent methylphosphate in several orientations. Their coplanar calculations correspond geometrically with our coplanar pSer−Lys and pSer−Arg orientations. Although the authors conclude that phosphate interactions with Lys are generally stronger than with Arg, their PM3−SM3 calculations show interaction free energies of +6.1 kcal/mol with coplanar $pSer^{-1}$−Lys and +3.6 kcal/mol for coplanar $pSer^{-1}$−Arg. The authors also found that $phenylphosphate^{-2}$ in complex with Lys or Arg produces an interaction free energy stronger than −28.0 kcal/mol in both cases. The findings clearly contradict our results, those generated both using molecular mechanics and using quantum mechanical methods, which are largely consistent with each other. It should be noted that the authors of this study speculated that the semiempirical quantum mechanical model may not have been well parametrized for phosphate groups.

Luo et al.[14] computed strengths of salt bridge interactions for Arg and Lys with phosphate using the CHARMM 22.0 empirical force field and a generalized Born implicit solvent model. In particular, they computed a PMF between monovalent phosphate and guanidinium that corresponds geometrically to our coplanar $pSer^{-1}$−Arg orientation. The authors found a contact minimum of about −3.8 kcal/mol, less than one-half the depth of our contact minimum of −9.3 kcal/mol for $pSer^{-1}$−Arg. Several differences in simulation protocol may contribute to this discrepancy. The CHARMM force field places a weaker charge on the unprotonated phosphate oxygens (−0.82*e*) than the charge we obtained from electrostatic potential fitting (−1.032*e*). Further, the authors used the protonated phosphate oxygen to accept one of the planar hydrogen bonds, while we used deprotonated oxygens to accept both hydrogen bonds. Additionally, because the authors were trying to mimic experiments involving ion pairs in high ionic strength (1 mol/L) aqueous solution, they applied an ionic shielding correction to their ion pair calculations that weakened their interactions on the order of 1 kcal/mol. Finally, the authors used a generalized Born implicit solvent model instead of Poisson−Boltzmann and explicit solvent used here.

Some efforts have also aimed to quantify the strengths of phosphate interactions with charged side-chain analogues experimentally. Springs and Haake[68] extracted free energies of association for guanidinium−phosphate and butylamine−phosphate from pK_a shifts. The absolute free energies cannot be directly compared to our work, because the experimental free energies are for free ions, whereas the computational PMFs represent constrained geometries, which is more appropriate to understanding hydrogen bonding in a macromolecule. In addition, the experiments were carried out in solution with 1 mol/L ionic strength, creating significant ionic shielding. However, the relative free energies can be profitably compared. Specifically, the experimentally determined free energies show a stronger interaction for guanidinium−phosphate (−0.6 kcal/mol) than butylamine−phosphate (−0.4 kcal/mol), in agreement with our results.

Salt Bridge Interactions of pAsp. Response regulators in bacterial "two component" signaling systems use Asp side chains to accept a phosphate group from a sensor histidine kinase.[69] Resonance structures involving the π orbitals of the covalently linked carboxylate and phosphate groups suggest that the electron density on the phosphate group on pAsp may be significantly different from that of pSer/pThr. (A similar argument could be made regarding pTyr, i.e., that there could be some conjugation between the π electronic systems in the benzene ring and on the phosphate. However, quantum calculations on benzyl phosphate followed by electrostatic potential fitting (see Materials and Methods) suggested that the electron density on the phosphate group in pTyr is minimally different than that on methyl phosphate (pSer), and we did not pursue this issue further.) This conjecture is confirmed by the partial charges we obtained by electrostatic potential fitting, as discussed in the Materials and Methods. We examined the effect of this difference on hydrogen-bond strengths with the panel of hydrogen-bond donors.

As with propionic acid (Glu) and methyl phosphate (pSer) acceptors, the energies for acetyl phosphate (pAsp) with propyl guanidinium (Arg) and butyl ammonium (Lys) in a collinear approach are very similar (within 1 kcal/mol). The more striking comparison arises from different charge states of pAsp. Deprotonating pAsp when accepting from collinear Lys stabilizes the interaction by −1.4 kcal/mol, and by −1.5 kcal/mol when the donor is Arg. In contrast, deprotonating pSer in a collinear salt bridge stabilizes the interaction by only −0.5 kcal/mol with Lys and −1.0 kcal/mol with Arg. The deprotonation effect increases in the coplanar approach only for lysine. Coplanar $pAsp^{-2}$−Lys shows a −2.5 kcal/mol stabilization over $pAsp^{-1}$−Lys, while coplanar $pAsp^{-2}$−Arg yields only a −1.0 kcal/mol stabilization over $pAsp^{-1}$−Arg. Bidentate hydrogen bonding continues to produce strong effects, with coplanar Arg showing a −3.3 kcal/mol stronger salt bridge than a collinear approach with $pAsp^{-1}$ and a −2.8 kcal/mol stronger interaction than collinear with $pAsp^{-2}$. Coplanar Arg also bonds stronger than coplanar Lys to pAsp in the −1 and −2 charge states by −3.9 and −2.4 kcal/mol, respectively, as Lys cannot form bidentate bonds due to the same geometric constraints inhibiting them with Glu and pSer acceptors.

The greater sensitivity to charge state of pAsp over pSer might be attributed to differences in the charge distribution for the −1 and −2 ions. The quantum mechanically calculated partial charges for the acceptor oxygens on pSer remain at −1.032*e* regardless of protonation of the remaining phosphate oxygen. In contrast, partial charges of the corresponding oxygens of pAsp decrease to −1.016*e* from −0.949*e* upon phosphate deprotonation. We attribute these differences in partial charges to protonation effects on electron density due to resonance between the carboxylate and phosphate π-electron systems; this effect of course does not occur in methyl phosphate (pSer).

Hydrogen-Bond Interactions with Amide NH Groups. An earlier survey (data not shown) identified backbone amides as the second most common hydrogen-bond partner after Arg with phosphates in phosphorylated proteins in the Protein Data Bank.[70] We used *N*-methylacetamide (CH_3−NH−CO−CH_3) as

(67) Cramer, C. J.; Truhlar, D. G. *J. Comput.-Aided Mol. Des.* **1992**, *6*, 629−666.
(68) Springs, B.; Haake, P. *Bioorg. Chem.* **1977**, *6*, 181−190.
(69) Hoch, J. A.; Silhavy, T. J. *Two-Component Signal Transduction*; ASM Press: Washington, DC, 1995.
(70) Berman, H. M.; Westbrook, J.; Feng, Z.; Gilliland, G.; Bhat, T. N.; Weissig, H.; Shindyalov, I. N.; Bourne, P. E. *Nucleic Acids Res.* **2000**, *28*, 235−42.

Table 2. Hydrogen-Bonding Free Energies in kcal/mol Computed from Continuum Electrostatics

	Lys collinear	Arg collinear	Lys coplanar	Arg coplanar	amide NH collinear
Glu	−5.1	−3.9	−2.7	−10.6	−2.3
pSer(−1)	−6.7	−6.1	−3.6	−13.0	−2.1
pSer(−2)	−7.7	−6.7	−5.6	−15.4	−1.2
pAsp(−1)	−5.5	−5.1	−2.4	−10.8	−2.6
pAsp(−2)	−7.2	−6.5	−5.8	−15.5	−1.3

Table 3. Hydrogen-Bonding Free Energies in kcal/mol Computed from SCRF Quantum Mechanics

	Lys collinear	Arg collinear	Lys coplanar	Arg coplanar	amide NH collinear
Glu	−4.5	−3.7	−4.3	−10.2	−2.1
pSer(−1)	−4.4	−4.1	−2.5	−8.1	−0.8
pSer(−2)	−8.6	−6.8	−8.8	−13.6	−2.6
pAsp(−1)	−3.8	−3.5	−2.4	−8.2	−0.8
pAsp(−2)	−7.8	−6.4	−8.5	−12.6	−2.7

Table 4. Change in Salt Bridge Free Energy (kcal/mol) When a Carboxylate Is Substituted for a Phosphate[a]

ion pair	orientation	ΔΔ*G* with Glu acceptor
pAsp(−1)−Lys	collinear	0.1
pAsp(−1)−Lys	coplanar	−0.2
pAsp(−1)−Arg	collinear	−0.5
pAsp(−1)−Arg	coplanar	−2.2
pAsp(−2)−Arg	coplanar	−1.2
pSer(−1)−Arg	collinear	0.3

[a] Charged−charged ion pairs with carboxylate acceptor substitutions worth at least 0.5 kcal/mol as with a phosphate acceptor are shown.

an analogue of the protein backbone to investigate the free energy of backbone hydrogen bonds to the carboxylate and phosphate hydrogen-bond acceptors. In all simulations, the amide hydrogen was placed in a collinear geometry with its acceptor. The glutamate analogue was truncated to acetate because hydrophobic interactions were observed between the aliphatic tail of Glu and the methyl caps of *N*-methylacetamide. In contrast to the behavior observed with Arg or Lys donors, the interaction weakens slightly when the acceptor is deprotonated. A weakened hydrogen bond arising from a stronger P−O dipole may appear counterintuitive. However, hydrogen-bond formation depends on a delicate balance between the free energy gain of bonded pairs and the loss of hydrogen bonds to surrounding waters, and the desolvation penalty is significantly lower for the protonated phosphate group. This effect was also observed by Wong et al.[41] in a study involving phosphate−amide interactions with phosphate acceptors possessing both −1 and −2 charges.

Implicit Solvent Poisson−Boltzmann Calculations. While continuum solvent models can provide substantial speed advantages relative to explicit solvent in performing free energy calculations, the merits and shortcomings of implicit solvent models remain a subject of interest and some contention. Treating the solvent as a dielectric continuum neglects important first-shell solvation effects arising from the finite size and asymmetry of a water molecule.[18−20] In particular, the very strong ionic interactions between a −2 charged phosphate with positively charged ions presents a challenging test of implicit solvent models.

We performed Poisson−Boltzmann (PB) implicit solvent calculations on all configurations (see Materials and Methods) to compare with the explicit solvent MD simulations. We retained the same geometries, atomic radii, Lennard-Jones parameters, and partial charges in these calculations. Figure 2 shows one example of a comparison between the explicit solvent PMF and the implicit solvent results; the others are available in the Supporting Information. As has been seen in other work,[15,18] the implicit solvent potentials generally contain less structure than the explicit solvent PMFs, that is, no secondary minima, consistent with the fact that the implicit solvent model treats water as a continuum. In addition, we observe that the implicit solvent results tend to exaggerate the energy barrier required for separating the ions from contact to infinite separation.

Our primary concern here, however, is the depth of the contact minima (Table 2), and in this respect the implicit solvent results generally recapitulate most of the key trends observed in the explicit solvent PMFs. In particular, the implicit solvent results agree that protonating the phosphate group weakens hydrogen bonds with charged donors but strengthens interactions with the amide NH group, and that the strongest hydrogen bond of the phosphate group is the bidentate interaction with guanidinium. Overall, the implicit solvent calculations predict stronger hydrogen-bonding interactions of the phosphate group than explicit solvent MD, with the largest discrepancies observed for Arg forming bidentate interactions with unprotonated phosphate. It may be possible to reduce the general overprediction of the hydrogen-bond strengths by empirically adjusting the radii used to define the dielectric surface in the implicit solvent calculation, but we have not performed such an optimization at this time. It should also be reiterated that the explicit solvent PMFs cannot be considered to be free of error either and will depend on the choice of explicit solvent model and other simulation parameters.

Self-Consistent Reaction Field Quantum Mechanics Calculations. To investigate the possible effects of electronic polarization on the energetics of hydrogen bonding, we performed quantum mechanics (QM) calculations using a self-consistent reaction field to mimic the condensed phase (see Materials and Methods). One limitation of this method with respect to the MD calculations is the use of implicit solvent. An advantage, however, is that atomic partial charges are recomputed at each distance to account for electronic polarizability. For instance, the donated Arg hydrogens in the $pSer^{-2}$−Arg coplanar configuration increase in charge from 0.54*e* and 0.51*e* at 11.0 Å separation to 0.69*e* and 0.62*e* at the contact minimum distance of 4.25 Å.

As with the PB analysis, the QM calculations were carried out on fixed orientations at 0.25 Å intervals. The total interaction energies, computed from the difference between potentials at 11.0 Å separation and the contact minima, are presented in Table 3. A superposition of MD, PB, and QM energy landscapes is shown in Figure S3. As observed in the explicit solvent MD results, bidentate hydrogen bonds with coplanar arginine tend to produce salt bridges about twice as strong as the monodentate collinear approach. On average, QM found 1.5 kcal/mol stronger interactions than MD with a fixed charge force field and explicit solvent. The largest differences occur for configurations with a −2 charged receptor. The mean difference in free energy between QM and MD for −2 charged receptors is −3.1 kcal/

mol, while the same figure for −1 charged receptors is −0.9 kcal/mol. It is of course reasonable that the larger charge on the −2 anions would induce larger polarization effects.

Because the quantum mechanical and PB calculations both employ an implicit solvent model, it is informative to compare trends between these methods as well. The average difference between QM and PB is −1.4 kcal/mol, similar to the difference observed when comparing to MD. As expected, the QM calculations are substantially more sensitive to polarization effects than PB. The mean free energy difference between QM and PB for −2 charged receptors is −3.0 kcal/mol, while for −1 charged receptors it is 1.0 kcal/mol.

Overall, the quantum mechanical calculations show a significant role for polarization in hydrogen-bond stability and suggest that the explicit solvent molecular dynamics simulations, using a fixed charge force field, might systematically underestimate the strengths of hydrogen bonds involving the phosphate group with a −2 charge, relative to −1 phosphate or carboxylate groups. Generally, the quantum mechanical calculations support the conclusions from the explicit solvent molecular dynamics. One key limitation of the quantum calculations, however, is that solvent is treated as a dielectric continuum, as in the implicit solvent results. Quantum mechanical simulations are possible with explicit solvent, but extensive sampling of the water is required to obtain reasonable free energies of solvation, making this approach computationally extremely intensive. A more tractable way to assess electronic polarizability effects in explicit solvent may be to perform molecular dynamics using the new generation of polarizable force fields[71] with polarizable explicit water.[72]

Conclusions

Calculating hydrogen-bond free energies using multiple levels of theory has provided an internally consistent survey of hydrogen-bond strengths for common hydrogen-bonding partners, charge states, and geometries involving phosphorylated amino acid side chains. Additionally, the results suggest relative merits and shortcomings of each level of theory for this application. We conclude now by returning to the issues raised in the introduction.

(1) The first issue concerns the conditions under which Arg or Lys make stronger hydrogen bonds with a phosphorylated side chain. Lys forms as strong or slightly stronger hydrogen bonds than Arg with most of the acceptors studied in the collinear approach, probably because the ϵ-amino group of lysine has a denser positive charge field than the arginine guanidinium moiety. However, the results are unambiguous that the bidentate interactions available to guanidinium (Arg) with phosphate provide much stronger interactions than can be formed between ammonium ions (Lys) and phosphate in either a monodentate or a bidentate geometry.

(2) The next issue is the effect of phosphate protonation state on hydrogen-bond strength. Phosphate protonation (i.e., to the −1 charge state) produces a small but significant destabilizing effect with Arg and Lys donors (∼1 kcal/mol for pSer), particularly when the acceptor is pAsp (up to 2.5 kcal/mol). In contrast, the interactions with the amide NH group were mildly stabilized by acceptor protonation (∼0.6 kcal/mol); this is consistent with previous work of Wong et al.[41] Altogether, however, the hydrogen-bond strengths of the phosphate groups in the −2 and −1 charge states are strikingly similar. This is remarkable because the hydrogen-bond strength results largely from near-cancellation of two very large quantities: the strong Coulombic attraction between the ions, and the dielectric screening (and first-shell solvation effects) exerted by the water. Changing the charge state of the phosphate ion perturbs both of these quantities significantly, but apparently the changes are such that the overall strengths of the hydrogen bonds are not greatly affected.

(3) The final issue concerns the energetic consequences of substituting a carboxylate for a phosphate. All of the $pSer^{-2}$ orientations with charged residue donors form stronger salt bridges than these charged residue donors do with glutamate, suggesting that Asp/Glu substitution might not mimic phosphorylation. In contrast, the strengths of the hydrogen bonds of the phosphate groups in the −1 charge state are generally closer to the corresponding hydrogen bonds of the carboxylate group, especially for $pAsp^{-1}$. Table 4 lists hydrogens bonds with phosphate acceptors that are at least 0.5 kcal/mol as strong when the acceptor is a carboxylate. Of course, in the protein microenvironment, the local electrostatic field, steric restrictions, exposure to various solvent and ion concentrations, departure from ideal orientations, and other factors will significantly impact the hydrogen-bond strengths computed here.

Nevertheless, these calculations provide a quantitative framework for beginning to assess when substitution with Glu or Asp might mimic phosphorylation, at least when a protein structure is available, and suggest that the protonation state of the phosphate may be a critical parameter.

Acknowledgment. This work was funded by an NSF CAREER Award to M.P.J. (MCB-0346399) and start-up funds provided by HHMI Biomedical Research Support Program grant #5300246 to the UCSF School of Medicine. D.J.M. was supported by a graduate fellowship from the ARCS Foundation and NIH Training Grant GM067547, I.C. by a postdoctoral fellowship from the Alfred P. Sloan Foundation, E.S.G. by a graduate fellowship provided by the Burroughs Wellcome Interfaces of Science Program and NIH Training Grant GM08284, and S.EW. by a UC President's Dissertation-Year Fellowship. M.P.J. is a consultant to Schrodinger Inc.

Supporting Information Available: Partial atomic charges and OPLS atom types used in the calculations; explicit solvent PMF for the NaCl control calculation; sample PMF using the quantum SCRF method, as compared to implicit and explicit solvent molecular mechanics results; and explicit and implicit solvent PMFs for all 25 hydrogen-bonding interactions, with insets depicting the geometries. This material is available free of charge via the Internet at http://pubs.acs.org.

JA063019W

(71) Halgren, T. A.; Damm, W. *Curr. Opin. Struct. Biol.* **2001**, *11*, 236−242.
(72) Yu, H.; van Gunsteren, W. F. *J. Chem. Phys.* **2004**, *121*, 9549−9564.